*Desalination and Water Treatment*
www.deswater.com
doi: 10.5004/dwt.2020.25031

179 (2020) 280–287
March

# Application of response surface methodology for modeling and optimization of lead (Pb(II)) removal from seaweed extracts via electrodialysis

Xiaomeng Wang[a], Junjun Feng[a], Zhun Ma[a,*], Jianye Li[b,*], Dongmei Xu[a], Xiuju Wang[c], Yongchao Sun[a,d], Xueli Gao[d,*], Jun Gao[a]

[a]*College of Chemical and Environmental Engineering, Shandong University of Science and Technology, Qingdao 266590, China, Tel. +86-532-86057798; Fax: +86-532-86057798; email: mzyxy199@163.com (Z. Ma), Tel. +8615764237673; email: 15764237673@163.com (X. Wang), Tel. +8617852025852; email: 1178701904@qq.com (J. Feng), Tel. 8613589304512; email: xudongmei@sdust.edu.cn (D. Xu), Tel. +8617854259757; email: yongchao_sun@163.com (Y. Sun), Tel. +86-532-86057103; email: gao@sdust.edu.cn (J. Gao)*
[b]*School of Chemical and Environmental Engineering, Weifang University of Science & Technology, Shouguang 262700, China, Tel. +86-536-5106528; Fax: +86-536-5106528; email: ljy@techmoris.com (J. Li)*
[c]*Key Laboratory of Water Resources and Environmental Engineering in Universities of Shandong, University of Jinan, Jinan 250022, China, Tel. +86-531-89736378; email: chm_wangxj@ujn.edu.cn (X. Wang)*
[d]*Key Laboratory of Marine Chemistry Theory and Technology, Ministry of Education; College of Chemistry and Chemical Engineering, Ocean University of China, Qingdao 266100, China, Tel. +86-532-6678 6513; Fax: +86-532-6678 6513; email: gxl_ouc@126.com (X. Gao)*

Received 27 April 2019; Accepted 14 October 2019

## ABSTRACT

The Box–Behnken design response surface methodology (BBD-RSM) was utilized to model and optimize electrodialysis process for lead (Pb(II)) removal from seaweed extracts. The experiments were conducted with three influential variables including the operational voltage and initial lead concentration and flow rate using a full $2^4$ factorial experimental design. According to the ridge and canonical analysis, the effect of major factors on Pb(II) removal in ED process follows the order: operational voltage > flow rate > initial lead concentration. Under the optimized parameters, the lead removal of 76.52% was acquired which showed good agreement with model predicted (75.45%) result. The feasibility of RSM model for lead removal response was verified by analysis of variance (ANOVA), which indicated a good reproducibility and fit of the experimental data with a high value coefficient ($R^2 = 0.9945$ and $R^2_{adj} = 0.9874$). The results suggested that electrodialysis with Box–Behnken design response surface methodology is regarded as the promising technology for lead removal from seaweed extracts.

*Keywords:* Response surface methodology; Lead removal; Electrodialysis; Box–Behnken design; Seaweed extracts

## 1. Introduction

Seaweed is widely distributed in the ocean, and its extracts have demonstrated immense potential for biofuel production [1,2], nanocomposites [3], food [4,5], etc. Seaweeds have been promoted for their therapeutic capabilities, including antioxidant, anti-inflammatory, antiviral and antibacterial properties [6]. Seaweed extracts can also promote the growth of plants and strengthen the health of soil in agricultural applications [7], and has the effects of antitumor and anticancer in the medical field [8,9]. Although seaweed is a source of essential minerals, vitamins and

---

* Corresponding authors.

1944-3994/1944-3986 © 2020 Desalination Publications. All rights reserved.

antioxidants, they have a high absorption capacity that can lead to a high accumulation of toxic metals [5]. Nowadays, high concentrations of heavy metals in seaweed and other seafood products have become a thorny problem as the result of more and more serious pollution of heavy metals to the oceans [10]. Lead is considered as one of the most toxic metals as the result of its persistent and irreversible damage to people and live organisms [11–13]. Kelp and seaweed are main sources of sodium alginate. The seaweed extracts containing lead ions cannot be directly used for the further processing of food and daily chemicals. The intake of lead ions, even the concentration is at a notably low level (15 μg/L), can cause a series of serious and long-term human health problems such as poisoning, anemia, brain hemorrhage, renal impairment, neurological disorders and even death [13–16]. Therefore, removal of heavy metal from seaweed extracts has become an urgent problem to be solved [16].

Numerous conventional physicochemical techniques were developed for the removal of lead (Pb(II)) from aqueous solution such as extraction [17], adsorption [18,19], chemical precipitation [20], coagulation [20–22], and ion exchange [23]. However, most of the processes are not cost-effective and have limitations such as long operating time and potential contamination caused by the chemical additives [24–27]. Membrane separation technology is a non-polluting separation process that competes with the above-mentioned processes of the lead removal of aqueous solution [28,29]. Nowadays, many membrane technologies including reverse osmosis, nanofiltration [30], membrane distillation [31] and electrodialysis (ED) [24,32] were used to remove heavy metal from aqueous solution and wastewater. As a promising method of lead removal, ED process has been widely applied in heavy metal removal due to its selective desalination, low energy consumption, eco-friendliness and applicability to decentralized system [2]. The removal of lead by ED in synthetic aqueous solutions has been investigated by Gherasim et al. [24]. However, there is a dearth of literature for the lead (Pb(II)) removal from seaweed extracts via ED.

As a hybrid of mathematical and statistical strategy, response surface methodology (RSM) is widely utilized to acquire optimal operating parameters with minimum number of experiments and also to evaluate the interactive effects of possible influential factors on treatment efficiency [33–35]. Box–Behnken design (BBD), one of the most common spherical and revolving RSM designs, was employed to develop the design matrix which is made up of 17 experiments with five centre points and two replicates [36,37]. Recently, RSM involving BBD has been verified to be an effective approach in designing experiments, developing empirical models and establishing optimal process variables in environmental, chemical engineering, material synthetic, and biological experimental processes [38–41]. However, as far as we are concerned, the literature regarding the optimization and modeling on the interactive effects of the operating parameters on Pb(II) removal applying by ED process based on RSM from seaweed extracts are scarce.

In this study, for the first time, RSM using Design-Expert 10.0.3 Trial software based on BBD was employed to optimize operational variables and investigate individual and interactive effects of influential factors on Pb(II) removal from seaweed extracts by ED process. In a perspective of optimization, the percentage of Pb(II) removal has been evaluated in terms of statistical experimental design. The quadratic polynomial regression models involving three operational variables such as operating voltage, flow rate, initial concentration of Pb(II), and taking the removal of Pb(II) as the major response were successfully developed. The goodness of fit of the model and the significance of influential factors were validated by means of the analysis of variance (ANOVA).

## 2. Materials and methods

### *2.1. Materials*

The sodium alginate, as the seaweed extract, was purchased from Qingdao Bright Moon Seaweed Group Co., Ltd., China. Lead chloride, glucose, sodium sulfate, nitric acid, hydrochloric acid and lead nitrate were of analytical grade and provided by Chengdu Chron Chemicals Co., Ltd., China. Deionized water was used throughout all experiments.

### *2.2. Electrodialysis system*

The ED experiments were conducted by a commercial laboratory scale TRBP3010-I unit (Beijing Tingrun Membrane Technology Co., Ltd., China). The ED system contains 16 pieces of anion exchange membranes and 15 pieces of cation exchange membranes (manufactured by Beijing Tingrun Membrane Technology Co., Ltd., China). The dimensions of the membranes were 100 mm × 300 mm × 0.21 mm with the effective surface area for each membrane of 150 $cm^2$. The main properties of membranes such as thickness, burst strength, IEC, resistance and transport number are listed in Table 1. These membranes were separated by polypropylene plastic sheet flow mesh spacers with the dimensions for each plastic sheet of 300 mm × 100 mm × 0.85 mm. The polypropylene loop-less baffle consisted of baffle frame and baffle net, comprising inlet and outlet water distribution hole, sealing perimeter, water distribution tank and grid section. The spacers can support the membrane and form stack's compartments which can promote turbulent flow of stream. The ED equipment equipped three cylindrical reservoirs for electrode rinsing, dilute and concentrate solution allowing for continuous circulation by centrifugal pumps [28,42]. Furthermore, the stack comprises a programmable DC power supply (PS-305DM, Longwei Instruments (HK) Co., Ltd.) with automatic voltage regulation on ED module in the range of 0–30 V. The DC power supply device was connected to module through ruthenium-coated titanium electrode and stainless-steel electrode. The cathode plate and the anode plate are, respectively, located on both sides of the stack. A 0.05 M $Na_2SO_4$ solution was circulated between the anolyte and catholyte compartments. A single experimental run was carried out for 50 min. All the experiment runs were performed at ambient temperature 25°C ± 0.5°C.

### *2.3. Experimental procedure*

In this work, the schematic of ED process is presented in Fig. 1. Synthetic solutions containing seaweed extracts and Pb(II) were prepared by dissolving reagent grade sodium alginate and $PbCl_2$ into deionized water as feed solution

Table 1
Properties of membranes used for experiments

| Type | Thickness (μm) | Burst strength (kPa) | IEC (mmol/g) | Resistance (Ω-cm$^2$) | Transport number |
|---|---|---|---|---|---|
| Cation exchange membrane (JCM-II-05) | 160–230 | >250 | 2.0–2.9 | 1–3 | 95–99 |
| Anion exchange membrane (JAM-II-05) | 160–230 | >250 | 1.8–2.2 | 4–8 | 90–95- |

*Note*: The resistance was tested in 0.5 mol/L NaCl environment; transport number was tested with Na$^+$ and Cl$^-$ as the target ions.

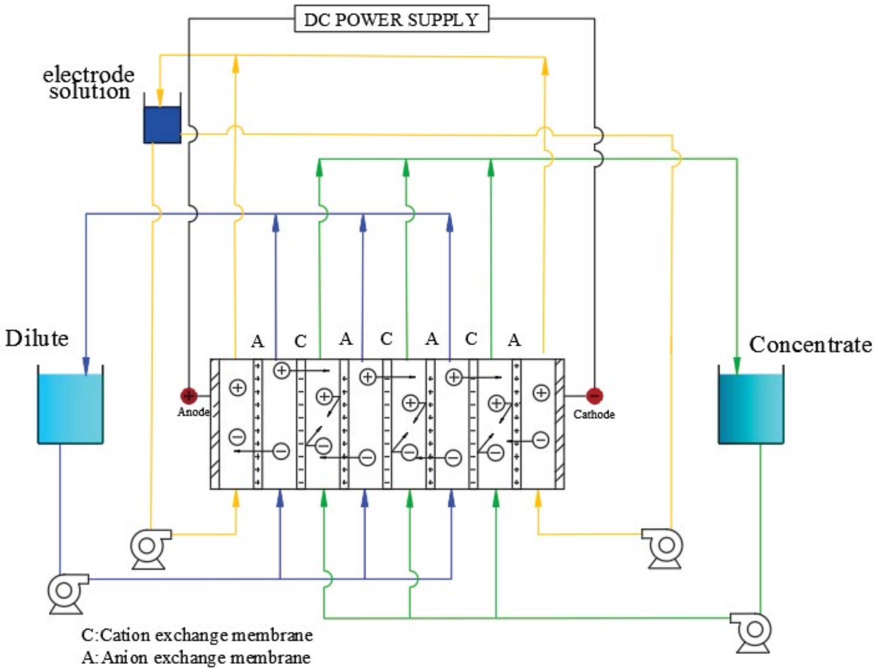

Fig. 1. Schematic illustration of electrodialysis process.

for the ED process. The concentrations of sodium alginate in actual solutions are variational and hence an average sodium alginate concentration of 0.17 g/L was used in all experiments. A few of glucose was added to the feed solutions to promote the dissolution of sodium alginate in water. In the present study, the effect of various parameters including flow rate (30, 60 and 90 L/h), operating voltage (5, 7 and 9 V) and initial concentration of lead (3, 5 and 7 mg/L) on the removal of Pb(II) from seaweed extracts were investigated. Based on the withstand voltage of each membrane, the upper limit of the voltage is selected by sum of withstand voltage of total membranes. The lower limit of voltage is selected by experiment. The dilute compartment and concentrate compartment were added with 1 L of feed solution, respectively. The feed solutions of diluted and concentrated compartments had same volume, initial components and concentration. Each compartment was connected to a separate external 5 L tank, allowing for continuous circulation by four magnetic driving pumps. In order to determine removal efficiencies, samples were periodically taken from the dilute and concentrate compartment during ED process. After each experimental run, the ED system was carefully rinsed twice with hydrochloric acid solution (10%, v/v) for a few minutes and several times with deionized water. Experiments were carried out according to the experimental scheme in Table 2. The concentrations of lead in dilute concentrate solutions were measured by flame atomic absorption spectrophotometer (TAS-986F, Beijing Purkinje General Instrument Co., Ltd., China) at a wavelength of 283.3 nm. The solutions were filtered using 0.45 μm PVDF filter (Millipore). Three repetitions were performed for all the analysis. The conductivity and pH of the dilute and concentrate compartment solutions were surveyed during the whole process by a conductivity meter (DDC-307, Shanghai INESA & Scientific Instrument Co. Ltd., China) and a pH meter (PHS-3E, Shanghai INESA & Scientific Instrument Co. Ltd., China), respectively.

### 2.4. Technical indicators of electrodialysis

The percentage removal of lead refers to the percentage of reduced lead concentration and initial lead concentration

Table 2
Box–Behnken design matrix for three variables together with the observed response

| | Coded values of the variable | | | |
|---|---|---|---|---|
| Experimental run | Factor 1 *A*: U (V) | Factor 2 *B*: c (mg/L) | Factor 3 *C*: v (L/h) | *Y* (%) |
| 1 | 9 | 5 | 90 | 65.8 |
| 2 | 7 | 3 | 90 | 67.0 |
| 3 | 7 | 5 | 60 | 75.1 |
| 4 | 7 | 5 | 60 | 75.1 |
| 5 | 7 | 5 | 60 | 75.9 |
| 6 | 9 | 5 | 30 | 62.4 |
| 7 | 7 | 3 | 30 | 64.1 |
| 8 | 7 | 7 | 30 | 65.9 |
| 9 | 5 | 3 | 60 | 62.7 |
| 10 | 7 | 5 | 60 | 75.1 |
| 11 | 5 | 5 | 90 | 62.4 |
| 12 | 5 | 5 | 30 | 60.7 |
| 13 | 9 | 3 | 60 | 64.1 |
| 14 | 7 | 5 | 60 | 75.1 |
| 15 | 9 | 7 | 90 | 65.3 |
| 16 | 7 | 7 | 90 | 67.7 |
| 17 | 5 | 7 | 60 | 61.0 |

and reflects the efficiency of the ED. The percentage removal of lead is defined as:

$$F = \frac{C_1 - C_0}{C_1} \times 100 \quad (1)$$

where $F$ is the percentage removal of lead, $C_0$ and $C_1$ are lead concentration of 0 min and $t$ min, respectively.

### 2.5. Box–Behnken design

The three variables of applied voltage ($A$), initial lead concentration ($B$) and flow rate ($C$) were selected based on the preliminary single-factor experiments. The experiment was carried out with different operating parameters such as flow rate (30, 60 and 90 L/h), operating voltage (5, 7 and 9 V) and initial concentration of lead (3, 5 and 7 mg/L). The BBD method was utilized to discuss the interaction and individual influences of three factors, so as to obtain the optimal lead desalination efficiency and its corresponding variable value. The BBD contained three levels for each factor which: the centre points (coded 0), the high level (+1) and the low level (–1). According to the BBD model, a total of 17 points was chosen to find optimum settings for three variables that result in maximum responses (optimal percentage removal of lead, $Y$). In this study, the experimental plan was determined by Design-Expert 10.0.3. The actual experimental design matrix of lead removal is given in Table 2. The value of each $Y$ represents the average of the identical experiments performed. In order to assure the reproducibility of the results, each experiment was performed at least two times.

Considering all the linear terms, square terms and linear by linear interaction items, the quadratic response model can be described as:

$$Y = \beta_0 + \sum \beta_i x_i + \sum \beta_{ii} x_{ii}^2 + \sum \beta_{ij} x_i x_j \quad (2)$$

where $Y$ is the predicted response surface function (percentage lead removal), $\beta_0$ is the model constant, $\beta_i$, $\beta_{ii}$ and $\beta_{ij}$ are the linear, quadratic and interaction constant coefficients, respectively. $x_i$ ($i$ = 1, 2, 3) and $x_j$ ($j$ = 1, 2, 3) represent the coded independent factors.

## 3. Results and discussion

### 3.1. Model fitting to responses of lead removal

The performance of ED investigated under various process conditions was investigated here with the aim to optimize the process by selecting the most convenient operating parameters. The levels of factors (voltage, initial concentration and flow rate) and the influence of their interactions on the lead removal are determined by means of the Box–Behnken design of response surface method. Experiments are finished for 17 experimental combinations, which consist of 12 trials and 5 center points, of the conditions selected by statistically designed experiments. An empirical relationship, which fits between the input variables and the data, is represented by a regression equation with interaction terms. The data are given from Box–Behnken design model. The final obtained equation (Eq. (3)) in terms of the coded factor is:

$$\begin{aligned} Y(\%) = {} & 75.20 + 1.76 \times A + 0.66 \times B + 1.30 \times C + 1.55 \times AB + \\ & 0.57 \times AC - 0.13 \times BC - 7.26 \times A^2 - 3.91 \times B^2 - 5.04 \times C^2 \quad (3) \end{aligned}$$

Table 3 shows the model $F$-value of 140.75, which implies that the model is significant [40]. The values of "Prob > $F$" less than 0.0001 indicate that the model terms are extremely significant, less than 0.05 and greater than 0.001 indicate model terms are significant, greater than 0.05 indicate model terms are not significant. The lack of fit $F$-value greater than 0.05 implies the lack of fit is not significant relative to the pure error [43]. Predicted $R^2$ is the judging indexes of how good the model predicts a response value. The predicted $R^2$ and adjusted $R^2$ should be within approximately 0.20 of each other to be in reasonable agreement [44]. In our case, the predicted $R^2$ of 0.9227 was in reasonable agreement with the adjusted $R^2$ of 0.9874, demonstrating the suitability of the model.

The $p$-values are utilized to examine the significance of each coefficient, which in turn might demonstrate the pattern of the interactions between the variables. It is showed that the coefficients ($A$, $B$, $C$, $AB$) are significant. The other term coefficients are not significant.

In this case, the normality of residuals is checked by analyzing the data. Fig. 2a shows the normal probability plot of these residuals. The distribution of points pretty close to a straight line indicates that the data were reasonable [22]. The model adequacy can be judged on diagnostic plots such as actual response and predicted response. It is showed that the

Table 3
ANOVA for response surface reduced quadratic model

| Source | Sum of squares | df | Mean squares | *F*-value | *p*-value |
|---|---|---|---|---|---|
| Model | 495.85 | 9 | 55.09 | 140.75 | <0.0001 |
| *A* | 22.36 | 1 | 22.36 | 57.11 | 0.0001 |
| *B* | 3.15 | 1 | 3.15 | 8.05 | 0.0252 |
| *C* | 13.96 | 1 | 13.98 | 35.65 | 0.0006 |
| *AB* | 7.85 | 1 | 7.71 | 20.06 | 0.0029 |
| *AC* | 1.41 | 1 | 1.33 | 3.60 | 0.0997 |
| *BC* | 0.068 | 1 | 0.060 | 0.17 | 0.6902 |
| $A^2$ | 207.75 | 1 | 207.15 | 530.73 | <0.0001 |
| $B^2$ | 60.31 | 1 | 60.17 | 154.08 | <0.0001 |
| $C^2$ | 87,54 | 1 | 89.49 | 223.64 | <0.0001 |
| Residual | 2.74 | 7 | 0.40 | | |
| Lack of fit | 2.23 | 3 | 0.77 | 5.80 | 0.0612 |
| Pure error | 0.51 | 4 | 0.13 | | |
| Cor. total | 498.59 | 16 | | | |

data points form fairly straight line and the residuals are distributed relatively near to the diagonal line. The distribution of all plots in Fig. 3 revealed that the data are reasonable and the model can describe the lead removal process well.

### *3.2. Effects of interactive variables on the removal efficiency of lead*

The interaction of voltage corresponds with flow rate and initial lead concentration is shown in Figs. 3b and c. Considering safety, potentiostatic mode is employed in this experiment which has advantage over galvanostatic mode. When the dilute concentration reaches a low value, the potentiostatic mode will limit the generation of high voltages, which protects the membranes. With the driving force of voltage, the anion and cation will get through the ion exchange membrane achieving the result of solution concentration or desalination [2]. It can be seen that the increase in voltage promotes the lead ions transfer. The relationship between lead flux and voltage is parabola, which agrees with the key respective contributions to migration of salt under current via electro-osmosis. This phenomenon is different from the linear relation of Le Han and Jia Wei Chew's findings [2,24], which is due to the limiting current density. Excessive voltage cannot promote the efficiency of lead removal and will increase the risk of scaling and precipitation, which will greatly shorten the life time of the membranes [29]. The results are given in Figs. 3b and c, which show the effects of different voltages on the variation of lead concentration. The lead concentration is high at the onset of the experiments with small resistance and large driving force of the mass transfer, so that migration speed is accompanied by a fast desalting speed of the lead removal [29]. However, with the lead removal, the resistance of the entire ED continues to increase but current decreases, and thus reduces the speed of lead removal [38]. And there is a maximum lead removal percentage when the operating voltage is set as 7.27 V. The reason is due to the higher ion permeate flux at larger voltage. Moreover, compared with range from 5 to 7.27 V, the removal efficiency of lead decreases when the voltage exceeds 7.27 V at same operating time. Compared with Gherasim et al.'s [24] research, this ED process also shows ideal lead removal performance under lower voltage. The high voltage takes the responsibility for the occurrence of concentration polarization, which limits the process of ion transferring through the membrane. The ions transport between solution and membrane caused the decrease of the lead concentration on the dilute side and increase on the concentrate side near the membrane establishing a concentration profiles and building up a boundary layer. The increase in resistance of boundary layer caused by concentration polarization phenomenon hinders lead ion transfer [2]. The suitable flow rate is an effective strategy to eliminate the consequence of concentration polarization phenomenon.

The flow rate of ED process is an important process condition. The ED experiments were performed in the flow rate range of 30–90 L/h. Figs. 3a and c show the influence of flow rate on removal efficiency of lead. The figures show that the

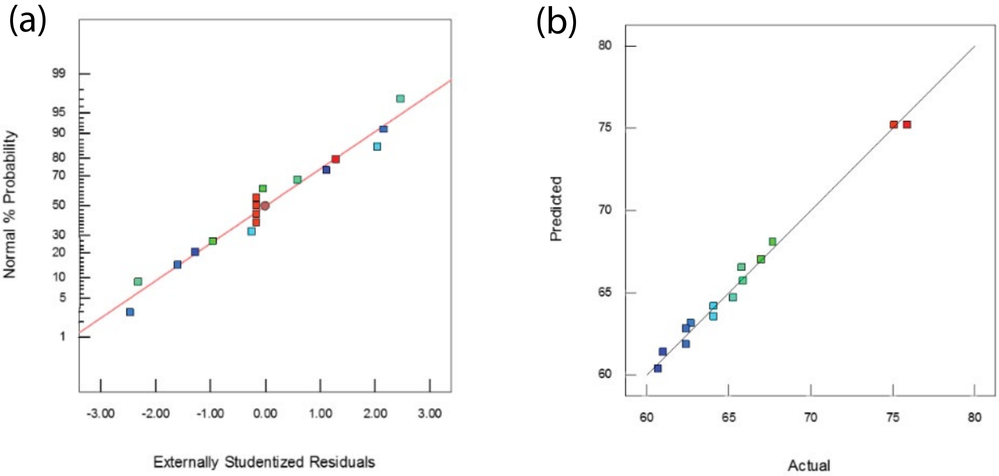

Fig. 2. Normal probability plot (a) and residual error (b) between the predicted response and actual response.

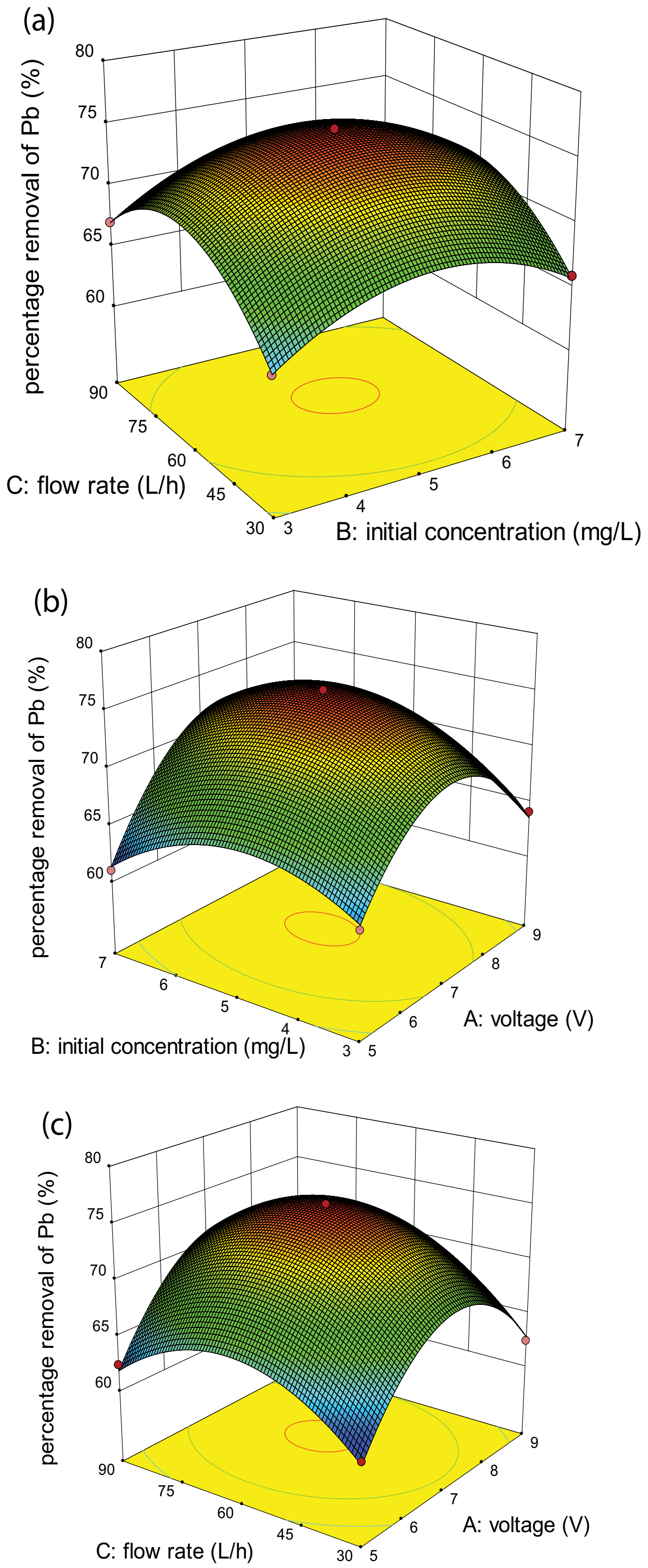

Fig. 3. Response surface plot: (a) the influence of initial concentration and flow rate on lead removal for the fixed voltage of 7 V; (b) the influence of initial concentration and voltage on lead removal for the fixed flow rate of 60 L/h; (c) the influence of flow rate and voltage on lead removal for the fixed initial lead concentration of 5 mg/L.

increase in flow rate promotes the lead removal of lead-containing aqueous solution under the range of flow rate from 30 to 70 L/h. However, the removal efficiency of lead decreases similar to a parabola with the increase in the flow rate from 60 to 90 L/h. The reason is that the thickness of the turbulence layer on both sides with the membrane decreases due to the increase in the flow rate. This reduced the resistance of the membrane itself, improved the current efficiency and reduced the energy consumption of the ED process [24]. However, the flow rate cannot be infinitely increased. The flow rate exceeding the allowable range of the membrane stack, a portion of the lead is washed away by the stream flow before it passes through the membrane. This phenomenon causes the lead removal efficiency is poor for the ED process. Excessive flow rate not only increases energy consumption but also damages the ion exchange membrane. Therefore, the appropriate choice of flow rate can properly reduce energy consumption, increase lead migration rate [24], and extend the service life of ion exchange membrane.

The initial lead concentration, which affects the applicability of ED process, is also an important ED parameter. The experiments are performed on various initial lead concentrations on the range of 3–7 mg Pb(II). Figs. 3a and b show the interactive influence of initial lead concentration on the removal efficiency of lead. The relationship between lead removal percentage and initial lead concentration is parabola [38]. At a range of initial lead concentration from 3 to 5.2 mg/L, the dilute concentration of lead is decreased rapidly. However, the processing capacity of the entire ED cannot deal with the increase in lead, and thus the percentage of lead removal cannot meet the requirements under high initial lead concentration. This deficiency can be met by multiple ED processes. With the migration of Pb(II), the ion transport between the solution and membrane results in a decrease in the Pb(II) concentration on the dilute side and an increase in the Pb(II) concentration on the other side near the membrane; this difference in concentration creates a boundary layer that increases the resistance of the dilute and slows down the rate of removal of the Pb(II) [2]. In view of this phenomenon, an appropriate increase in flow is the ideal way to deal with it [24].

According to the test and design of Box–Behnken response surface, the voltage, initial lead concentration and flow rate of feed solutions is stabilized in the values which are determined to be optimal for the ED, that is, 5.22 mg/L, 7.27 V and 64.06 L/h, respectively. Under the optimized parameters, the lead removal of 76.52% was acquired which showed good agreement with model predicted (75.45%) result. Compared with similar studies [2,24,30,45], the experimental results can guide the lead removal performance to meet the requirements. The experiment results are highly consistent with the predicted values, indicating BBD could be effectively applied to optimize the ED factors for the lead removal.

## 4. Conclusion

This work aimed to optimize experimental method of lead removal from seaweed extracts by ED using RSM and fit experimental data. The experiments contained a function of various operation parameters (initial lead concentration, flow rate and voltage). In order to examine the role of three operation factors (initial lead concentration, flow rate and voltage) on lead removal we used RSM by the Box–Behnken model. As can be seen, a second-order polynomial regression model could appropriately account for the experimental data onto coefficient of determination ($R^2$) value of 0.9945. The simultaneous optimization of the multi-response system by desirability function indicated that 76.52% removal of lead can be possible by using the optimal process parameters of initial lead concentration of 5.22 mg/L, voltage of 7.27 V and flow rate of 64.06 L/h. The fitting data of lead removal indicated that applied voltage and flow rate could significantly affect the lead removal from the seaweed extracts by ED. Operational voltage and time were the most significant factors that influenced energy consumption of ED. This work showed that the Box–Behnken model was suitable to optimize the experiments for lead removal from seaweed extracts by ED.

## Acknowledgments

This work was financially supported by the Key Research Project of Shandong Province (No. 2017CXGC1004), the National Natural Science Foundation of China (No. 21878178), Shandong Science and Technology Development Plan (No. 2018GGX107001) and Young Taishan Scholars Program of Shandong Province.

## References

[1] M.R. Tabassum, A. Xia, J.D. Murphy, Biomethane production from various segments of brown seaweed, Energy Convers. Manage., 174 (2018) 855–862.

[2] Y.L. Le Hana, Jia Wei Chew, Boron transfer during desalination by electrodialysis, J. Membr. Sci., 547 (2018) 64–72.

[3] T.A. Roseline, M. Murugan, M.P. Sudhakar, K. Arunkumar, Nanopesticidal potential of silver nanocomposites synthesized from the aqueous extracts of red seaweeds, Environ. Technol. Inno., 13 (2019) 82–93.

[4] K. Chen, M. Roca, Cooking effects on chlorophyll profile of the main edible seaweeds, Food Chem., 266 (2018) 368–374.

[5] S. Paz, C. Rubio, I. Frias, A.J. Gutierrez, D. Gonzalez-Weller, V. Martin, C. Revert, A. Hardisson, Toxic metals (Al, Cd, Pb and Hg) in the most consumed edible seaweeds in Europe, Chemosphere, 218 (2019) 879–884.

[6] A.C. Leri, M.R. Dunigan, R.L. Wenrich, B. Ravel, Particulate organohalogens in edible brown seaweeds, Food Chem., 272 (2019) 126–132.

[7] D. Battacharyya, M.Z. Babgohari, P. Rathor, B. Prithiviraj, Seaweed extracts as biostimulants in horticulture, Sci. Hortic.-Amsterdam, 196 (2015) 39–48.

[8] A.G. La Macchia Pedra, F. Ramlov, M. Maraschin, L. Hayashi, Cultivation of the red seaweed *Kappaphycus alvarezii* with effluents from shrimp cultivation and brown seaweed extract: effects on growth and secondary metabolism, Aquaculture, 479 (2017) 297–303.

[9] J. Jiang, S. Shi, Seaweeds and Cancer Prevention, 2018, pp. 269–290.

[10] K.D. Bastami, M.R. Neyestani, F. Shemirani, F. Soltani, S. Haghparast, A. Akbari, Heavy metal pollution assessment in relation to sediment properties in the coastal sediments of the southern Caspian Sea, Mar. Pollut. Bull., 92 (2015) 237–243.

[11] A.D. Davis, C.J. Webb, J.L. Sorensen, D.J. Dixon, R. Hudson, Geochemical thermodynamics of lead removal from water with limestone, Water Air Soil Pollut., 229 (2018) 177.

[12] A.J. Hargreaves, P. Vale, J. Whelan, L. Alibardi, C. Constantino, G. Dotro, E. Cartmell, P. Campo, Impacts of coagulation-flocculation treatment on the size distribution and bioavailability of trace metals (Cu, Pb, Ni, Zn) in municipal wastewater, Water Res., 128 (2018) 120–128.

[13] Y. Wu, M. Xu, J. Xue, K. Shi, M. Gu, Characterization and enhanced degradation potentials of biosurfactant-producing bacteria isolated from a marine environment, ACS Omega, 4 (2019) 1645–1651.

[14] A.A. Khan, U. Baig, Electrically conductive membrane of polyaniline–titanium(IV)phosphate cation exchange nanocomposite: applicable for detection of Pb(II) using its ion-selective electrode, J. Ind. Eng. Chem., 18 (2012) 1937–1944.

[15] N.A.H.M. Zaidi, L.B.L. Lim, A. Usman, Enhancing adsorption of Pb(II) from aqueous solution by NaOH and EDTA modified *Artocarpus odoratissimus* leaves, J. Environ. Chem. Eng., 6 (2018) 7172–7184.

[16] J. Xue, Y. Wu, K. Shi, X. Xiao, Y. Gao, L. Li, Y. Qiao, Study on the degradation performance and kinetics of immobilized cells in straw-alginate beads in marine environment, Bioresour. Technol., 280 (2019) 88–94.

[17] M.J. Aghagoli, F. Shemirani, Hybrid nanosheets composed of molybdenum disulfide and reduced graphene oxide for enhanced solid phase extraction of Pb(II) and Ni(II), Microchim. Acta, 184 (2016) 237–244.

[18] P. Pal, S.S. Syed, F. Banat, Gelatin-bentonite composite as reusable adsorbent for the removal of lead from aqueous solutions: Kinetic and equilibrium studies, J. Water Process Eng., 20 (2017) 40–50.

[19] S. Bao, K. Li, P. Ning, J. Peng, X. Jin, L. Tang, Highly effective removal of mercury and lead ions from wastewater by mercaptoamine-functionalised silica-coated magnetic nano-adsorbents: behaviours and mechanisms, Appl. Surf. Sci., 393 (2017) 457–466.

[20] A. Rabii, G.N. Bidhendi, N. Mehrdadi, Evaluation of lead and COD removal from lead octoate drier effluent by chemical precipitation, coagulation–flocculation, and potassium persulfate oxidation processes, Desal. Wat. Treat., 43 (2012) 1–7.

[21] J. Feng, Z. Yang, G. Zeng, J. Huang, H. Xu, Y. Zhang, S. Wei, L. Wang, The adsorption behavior and mechanism investigation of Pb(II) removal by flocculation using microbial flocculant GA1, Bioresour. Technol.. 148 (2013) 414–421.

[22] A. Assadi, M.M. Fazli, M.M. Emamjomeh, M. Ghasemi, Optimization of lead removal by electrocoagulation from aqueous solution using response surface methodology, Desal. Wat. Treat., 57 (2015) 9375–9382.

[23] E. Pehlivan, T. Altun, Ion-exchange of $Pb^{2+}$, $Cu^{2+}$, $Zn^{2+}$, $Cd^{2+}$, and $Ni^{2+}$ ions from aqueous solution by Lewatit CNP 80, J. Hazard. Mater., 140 (2007) 299–307.

[24] C.-V. Gherasim, J. Křivčík, P. Mikulášek, Investigation of batch electrodialysis process for removal of lead ions from aqueous solutions, Chem. Eng. J., 256 (2014) 324–334.

[25] R. Lafi, L. Gzara, R.H. Lajimi, A. Hafiane, Treatment of textile wastewater by a hybrid ultrafiltration/electrodialysis process, Chem. Eng. Process., 132 (2018) 105–113.

[26] Z. Ma, T. Lei, X. Ji, X. Gao, C. Gao, Submerged membrane bioreactor for vegetable oil wastewater treatment, Chem. Eng. Technol., 38 (2015) 101–109.

[27] J.S. Ho, Z. Ma, J. Qin, S.H. Sim, C.-S. Toh, Inline coagulation–ultrafiltration as the pretreatment for reverse osmosis brine treatment and recovery, Desalination, 365 (2015) 242–249.

[28] Z. Li, Z. Ma, Y. Xu, X. Wang, Y. Sun, R. Wang, J. Wang, X. Gao, J. Gao, Developing homogeneous ion exchange membranes derived from sulfonated polyethersulfone/N-phthaloyl-chitosan for improved hydrophilic and controllable porosity, Korean J. Chem. Eng., 35 (2018) 1716–1725.

[29] Y. Wang, C. Huang, T. Xu, Optimization of electrodialysis with bipolar membranes by using response surface methodology, J. Membr. Sci., 362 (2010) 249–254.

[30] A. Maher, M. Sadeghi, A. Moheb, Heavy metal elimination from drinking water using nanofiltration membrane technology and process optimization using response surface methodology, Desalination, 352 (2014) 166–173.

[31] H. Attia, S. Alexander, C.J. Wright, N. Hilal, Superhydrophobic electrospun membrane for heavy metals removal by air gap membrane distillation (AGMD), Desalination, 420 (2017) 318–329.

[32] S. Koushkbaghi, A. Zakialamdari, M. Pishnamazi, H.F. Ramandi, M. Aliabadi, M. Irani, Aminated-$Fe_3O_4$ nanoparticles filled chitosan/PVA/PES dual layers nanofibrous membrane for the removal of Cr(VI) and Pb(II) ions from aqueous solutions in adsorption and membrane processes, Chem. Eng. J., 337 (2018) 169–182.

[33] D. Liu, G. Gu, B. Wu, C. Wang, X. Chen, Degradation of isopropyl ethylthionocarbamate from aqueous solution by Fenton oxidation: RSM optimization, mechanisms, and kinetic analysis, Desal. Wat. Treat., 130 (2018) 87–97.

[34] H. Alidadi, A. Ghorbanian, M. Ghorbanian, E. Rahmanzadeh, N. Nemanifar, M. Mehrabpour, Evaluation of amoxicillin antibiotic removal by electrocoagulation process from aqueous solutions: optimization through response surface methodology, Desal. Wat. Treat., 132 (2018) 350–358.

[35] A.R. Rahmani, A. Shabanloo, M. Fazlzadeh, Y. Poureshgh, M. Vanaeitabar, Optimization of sonochemical decomposition of ciprofloxacin antibiotic in US/PS/nZVI process by CCD-RSM method, Desal. Wat. Treat., 145 (2019) 300–308.

[36] F. Mohammadi, F. Mohammadi, A. Esrafili, H.R. Sobhi, M. Behbahani, M. Kermani, E. Asgari, Z.R. Fasih, Evaluation of adsorption and removal of methylparaben from aqueous solutions using amino-functionalized magnetic nanoparticles as an efficient adsorbent: Optimization and modeling by response surface methodology (RSM), Desal. Wat. Treat., 103 (2018) 248–260.

[37] X. Deng, H. Zhou, X.-N. Qu, J. Long, P.-Q. Peng, H.-B. Hou, K.-L. Li, P. Zhang, B.-H. Liao, Optimization of Cd(II) removal from aqueous solution with modified corn straw biochar using Placket-Burman design and response surface methodology, Desal. Wat. Treat., 70 (2017) 210–219.

[38] X. Wang, N. Li, J. Li, J. Feng, Z. Ma, Y. Xu, Y. Sun, D. Xu, J. Wang, X. Gao, J. Gao, Fluoride removal from secondary effluent of the graphite industry using electrodialysis: optimization with response surface methodology, Front. Environ. Sci. Eng., 13 (2019) 51.

[39] P. Bhunia, S. Chatterjee, P. Rudra, S. De, Chelating polyacrylonitrile beads for removal of lead and cadmium from wastewater, Sep. Purif. Technol., 193 (2018) 202–213.

[40] Y. Guo, C. Wu, Q. Wang, M. Yang, Q. Huang, M. Magep, T. Zheng, Wastewater-nitrogen removal using polylactic acid/starch as carbon source: optimization of operating parameters using response surface methodology, Front. Environ. Sci. Eng., 10 (2016) 6.

[41] B.-H. Zhao, J. Chen, H.-Q. Yu, Z.-H. Hu, Z.-B. Yue, J. Li, Optimization of microwave pretreatment of lignocellulosic waste for enhancing methane production: hyacinth as an example, Front. Environ. Sci. Eng., 11 (2017) 17.

[42] N. Song, X. Gao, Z. Ma, X. Wang, Y. Wei, C. Gao, A review of graphene-based separation membrane: materials, characteristics, preparation and applications, Desalination, 437 (2018) 59–72.

[43] Z.D.I. Sktani, N.A. Rejab, M.M. Ratnam, Z.A. Ahmad, Fabrication of tougher ZTA ceramics with sustainable high hardness through (RSM) optimisation, Int. J. Refract. Met. Hard Mater., 74 (2018) 78–86.

[44] Y. Chan, M. Chong, C. Law, Optimization of thermophilic anaerobic-aerobic treatment system for Palm Oil Mill Effluent (POME), Front. Environ. Sci. Eng., 9 (2014) 334–351.

[45] K. Yetilmezsoy, S. Demirel, R.J. Vanderbei, Response surface modeling of Pb(II) removal from aqueous solution by *Pistacia vera* L.: Box-Behnken experimental design, J. Hazard. Mater., 171 (2009) 551–562.